# Advanced deep learning models based on neutrosophic logic for the analysis of brain tumor medical images

Dina Atef[1] and Doaa El Shahat[1]
[1]Department of Computer Science, Faculty of Computers and Informatics, Zagazig University, Zagazig 44519, Egypt
dinaatiff@fci.zu.edu.eg, debarakaat@fci.zu.edu.eg

## Abstract

The categorization of medical photographs poses considerable difficulties owing to noise, uncertainty, and ambiguous information. Conventional deep learning models frequently encounter difficulties in addressing this issue, resulting in diminished diagnostic precision, particularly in the context of low-quality or ambiguous situations. This work presents a hybrid methodology that combines Neutrosophic Set (NS) theory with deep learning models to improve magnetic resonance imaging (MRI) picture classification in uncertain settings. NS theory delineates three domains: True (T), Indeterminate (I) and False (F) to address picture uncertainty and noise, hence enhancing deep learning models' capacity to analyze complex, ambiguous visual data. To assess the methodology, four advanced deep learning models MobileNet, VGG16, DenseNet121 and InceptionV3 were employed, and their efficacy was analyzed on brain tumor medical image datasets. The findings demonstrate that models trained on NS-transformed data, especially DenseNet and inception, produce enhanced results relative to those trained on the original data, attaining notably higher accuracy, precision, and recall. This illustrates that integrating NS theory into deep learning models markedly improves their capacity to categorize uncertain and noisy MRI pictures, offering a reliable method for enhancing diagnostic accuracy in medical imaging.

**Keywords:** Deep Learning, Neutrosophic Set, Convolutional Neural Networks, MRI, Tumor Detection.

## 1. Introduction

With 9.6 million deaths in 2018, cancer ranks as the second most common cause of death globally. Comprising billions of cells, the sophisticated organ, known as the brain is responsible for the grouping of aberrant cells leading to brain tumors. These tumors could be benign or malignant; malignant tumors spread quickly to other parts of the brain. Various classifications of brain cancers exist, such as glioma, meningioma, and pituitary tumors [1]. MRI is a commonly employed method for visualizing the internal structures of the body through cross-sectional images. It offers comprehensive information about various tissues with excellent resolution and contrast, rendering it extensively utilized in the anatomical adjunctive assessment of brain tissue. MRI scans yield images of tissues exhibiting varying contrasts, facilitating precise diagnosis [2].

Computer-Aided Diagnosis (CAD) technologies are employed to expedite and enhance the accuracy of tumor detection for early illness identification. CAD systems can identify the tumor's location, kind, and severity, if applicable. Nevertheless, physicians' diagnoses are prone to inaccuracies, oversights, and delays owing to the vast volume of data. Because of this, the steps needed to classify, segment, localize, and find brain tumors have become the hardest parts of disease identification [3].

The term neutrosophy denotes the understanding of neutral thought, which constitutes the primary distinction between fuzzy logic and intuitionistic fuzzy logic and sets .The neutrosophic set possesses the necessary capabilities to serve as a comprehensive framework for uncertainty analysis in data sets, particularly in the realm of artificial intelligence and deep learning involving images [4]. In 1995, Smarandache came up with the idea of neutrosophic reasoning. After that, in 1999, its founder unified and made it more general. Neutrosophic logic has been used in many areas of computer science since then, such as pattern recognition, picture segmentation, and processing. It helps with a lot of study and real-world problems in many areas, like healthcare, economics, space satellites, and farming. There are a lot of new mathematical ideas that come from neutrosophy, including both classical and fuzzy ones.

The Neutrosophic Set (NS) theory provides a workable way to handle uncertainty in picture classification. In addition to T, F and I, it adds three more domains to normal binary logic. These groups show information that isn't complete, isn't regular, or isn't clear, which is common in medical MRI. NS theory emphasizes how reliable certain visual elements are while reducing the impact of areas that are unclear or noisy. It works by giving each item in a set one of three membership numbers (T, I, F), which show how much the item fits into the truth, indeterminacy, or falsehood domains [5]. When there isn't a lot of information or information that doesn't make sense, like in medical imaging, this three-part model is very helpful. The zones of uncertainty are clearly modeled in NS, which makes it a more advanced way to evaluate medical imaging. Still, not much study has been done on adding uncertainty management strategies like NS theory to the preprocessing or training pipeline of deep learning models. This means that uncertainty-aware methods for medical MRI interpretation are not widely used. This method uses the NS framework for MRI images, which makes classification easier by better representing image features and making the method more resilient in unclear situations [6]. The concepts of Artificial Intelligence (AI), Machine Learning (ML), and Deep Learning (DL) are individually distinct from one another

Generally, DL is a part of AI. ML is a methodology for data modeling and AI is a technology that is characterized by cognitive skills. Different types of ML approaches include reinforcement learning, supervised learning, and unsupervised learning. An increase in proficiency in speech recognition, picture analysis, object detection and disease diagnosis can be achieved through the use of DL [3]. It encompasses numerous categories, including Recurrent Neural Networks (RNN) and Convolutional Neural Networks (CNN). Convolution is implemented in CNNs, which are deep neural networks, as opposed to matrix multiplication. It gained recognition as a result of AlexNet, a 2012 model that exhibited exceptional performance in the ILSVRC. In the fields of computer vision and natural language processing, Convolutional Neural Networks (CNNs) are employed. Their architecture comprises concealed layers for feature extraction, with specific layers designated for feature extraction during training and others for classification. The overall efficacy and feature extraction are improved by the augmented hidden layer depth [7]. Four advanced deep learning models were employed for evaluation, including MobileNet, VGG16, DenseNet121, and InceptionV3. The findings from experiments indicate that models that were trained on NS-transformed data outperformed.

The subsequent sections of the paper are organized as follows. Section 2 delineates the literature review on the application of neural networks using deep learning techniques in medical domains, while section 3 clarifies the dataset employed and the deep learning methodologies implemented in this study. Section 4 outlines the experimental setting, presents the experimental data, and discusses the suggested models alongside other deep learning models for the detection. The endpoint of this work is situated in section 5.

## 2. Literature review

This part summarizes relevant studies on the use of NS functions with DL methods in image categorization. By means of the study of past studies, we want to identify shortcomings and constraints while stressing important findings, methods, and achievements in the integration of NS with DL models spanning several domains. Unsupervised approaches are becoming more and more important to researchers since they are so remarkably effective and able to independently generate features, hence reducing error rates. Medical image analysis requires deep learning models for segmentation, reconstruction, and classification as well as for other purposes.

In [8], the authors suggested an automatic segmentation approach for the identification of brain tumors utilizing MRI brain images. Convolutional Neural Networks (CNNs), machine learning algorithms inspired by biological processes, are under investigation for their application in brain tumor classification and radionics analysis. In [9], the researchers developed a useful brain tumor segmentation system including benign and malignant classification of brain tumors. The NS-EMFSE method helped to define brain tumors. CNN architectures—more especially, AlexNet—derived the features of the segmented images; later, SVM and KNN classifiers were used to identify them. Comprising feed-forward layers, CNN is a deep learning method. The authors Created an automatic detection method employing NS domain transformation, then implementing a process similar to that of a traditional CAD system within the NS domain [10]. A DCNN1 classifier was explicitly trained to recognize individual MCs and used as the phase for reducing false positive MCs.

In order to convert medical images from the grayscale spatial domain into the neutrosophic domain, the research makes use of the neutrosophic set theory [11]. True (T) images, indeterminacy (I) images, and falsity (F) images are the three types of images that can be found in the neutrosophic realm. Several different sources were utilized in the collection of the dataset that was utilized in this research. The dataset is divided into four distinct categories, which are as follows: COVID-19, normal, bacterial pneumonia, and viral pneumonia. An investigation into the influence that neutrosophic sets have on deep transfer learning models is the purpose of this study. Specifically, the deep learning models, such as AlexNet, GoogleNet, and ResNet18 are utilized in this investigation.

The study [12] made use of both picture and text data, and took inspiration from earlier techniques for embedding text onto photographs, with the intention of identifying the images through the application of neutrosophic classification algorithms. Neutrosophic convolutional neural networks, also known as NCNNs, are utilized for the purpose of acquiring feature representations of generated images for the purpose of classification objectives. It is necessary to demonstrate the utilization of a pipeline that makes use of NCNN in order to obtain representations of the unique fusion technique. Convolutional neural networks that are conventional are susceptible to unanticipated noisy scenarios during the testing process, which results in a decline in their performance when it comes to classifying noisy data. Positive results are obtained when our strategy is evaluated against a variety of sources using a multi-modal classification dataset.

A computer-aided diagnosis approach [13] was offered for categorizing malignant lesions whereby the acquired image undergoes first pre-processing using creative methods. Digital artifacts—including blood vessels and hair follicles—are deleted; then, using a novel histogram equalizing method, image improvement follows. The pre-processed image then moves through the segmentation procedure, during which the likely lesion is defined with the Neutrosophic technique.

Prior research has enhanced the application of NS in Deep Learning methodologies involving uncertainty and noise. Nonetheless, a requirement for robustness persists, and several of these investigations exhibit insufficient precision. Several more investigations were undertaken with a limited dataset, rendering the long-term effects uncertain.

## 3. Materials and Methods

This research utilizes NS domain photos to develop a transfer deep learning model aimed at classifying various types of brain tumors. Following this, the models are subjected to rigors testing, thorough evaluation, and detailed comparative analysis. This study will be carried out in a series of methodical steps, as depicted in figure 1, to analyze and evaluate the performance of various DL models on NS.

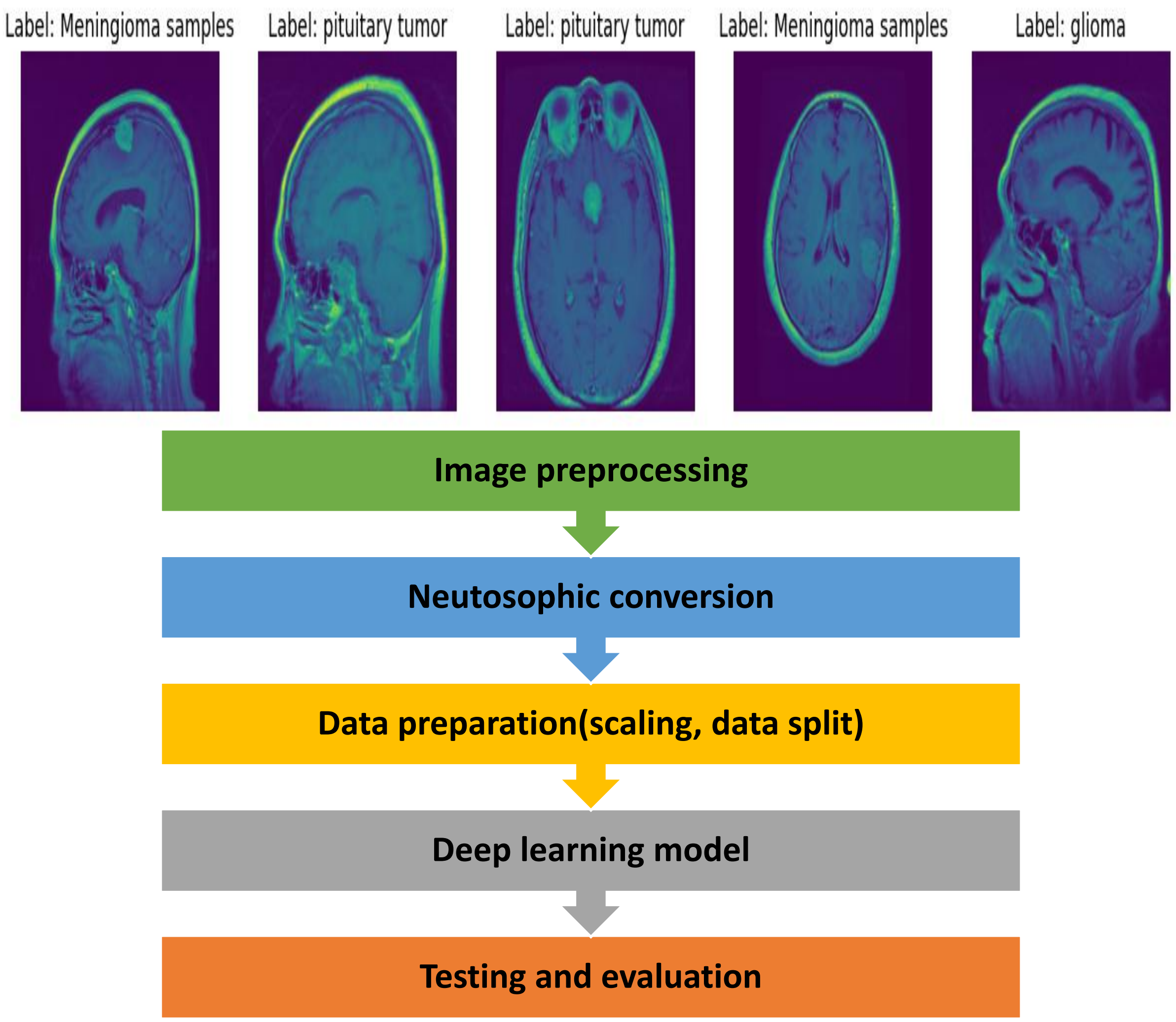


**Figure 1** Methodical steps of our study for various DL on NS

### *3.1 Dataset description*

The MRI dataset of the brain was collected from Nanfang Hospital in Guangzhou and General Hospital at Tianjin Medical University in China, spanning the years 2005 to 2010. The dataset consists of 3064 slices derived from 233 individuals, which includes 708 meningiomas, 1426 gliomas and 930 pituitary tumors. The images feature an in-plane resolution of 512×512, accompanied by a pixel size of 0.49×0.49 mm². The measurement of slice thickness is 6 mm, and the gap between slices is 1 mm. The tumor margin was meticulously delineated by three experienced radiologists [14]. The sample of dataset is displayed in figure 2.

**Figure 2** Dataset sample

### *3.2 Neuotrosphic set*

Neutrosophy (NS) is a sophisticated theoretical framework established by Florentin Smarandache [15]. NS represents a significant and advantageous concept within the context of computing fuzzy scenarios. As t changes within the T subsets, events in NS theory are classified into one of three sets: true (T) significance, where the status indicates the percentage of truth; indeterminacy (I) significance, where the status indicates the percentage of indeterminacy; and falsity (F) significance, where the status indicates the percentage of falsehood. In image processing, particularly in object and edge identification, all pixels of the image are classified into three subsets: T, I and F. The edge detection and object recognition processes of the image are then performed through necessary operations on these subsets. The input image undergoes transformation into the neutrosophic domain, as illustrated in Eqs. (1–5). The pixel P (q, r) in the picture domain is transformed into the NS $p_{NS}$ (q, r).

$$p_{NS}(\mathrm{q,r}) = \{\mathrm{T}_{q,r}, \mathrm{I}_{q,r}, \mathrm{F}_{q,r}\} \tag{1}$$

$$T(q,r) = \frac{\bar{N}(\mathrm{q,r}) - \bar{N}_{\min}}{\bar{N}_{\max} - \bar{N}_{\min}} \tag{2}$$

$$I(q,r) = 1 - \frac{\bar{H}(\mathrm{q,r}) - \bar{H}_{\min}}{\bar{H}_{\max} - \bar{H}_{\min}} \tag{3}$$

$$H(\mathrm{q,r}) = \mathrm{abs}(\mathrm{N(q,r)} - \mathrm{N}(\bar{\mathrm{q}},\mathrm{r})) \tag{4}$$

$$F(\mathrm{q,r}) = 1 - \mathrm{T(q,r)} \tag{5}$$

Where $N(q,r)$ denotes the gray value of the corresponding pixel, $\bar{N}(q,r)$ signifies the regional average value of $N(q,r)$ and $H(\mathrm{i,j})$ represents the homogeneity value, defined as the absolute difference between the intensity of $N(q,r)$ and its local mean value $\bar{N}(q,r)$. Upon converting the image to the NS domain, the brain tumor image should be retained in the (T) domain, while the edges are to be positioned in the (I) domain and the background layer should be located in the (F) domain. Figure 3 demonstrates the difference between the original image and the images following conversion into NS image domains.

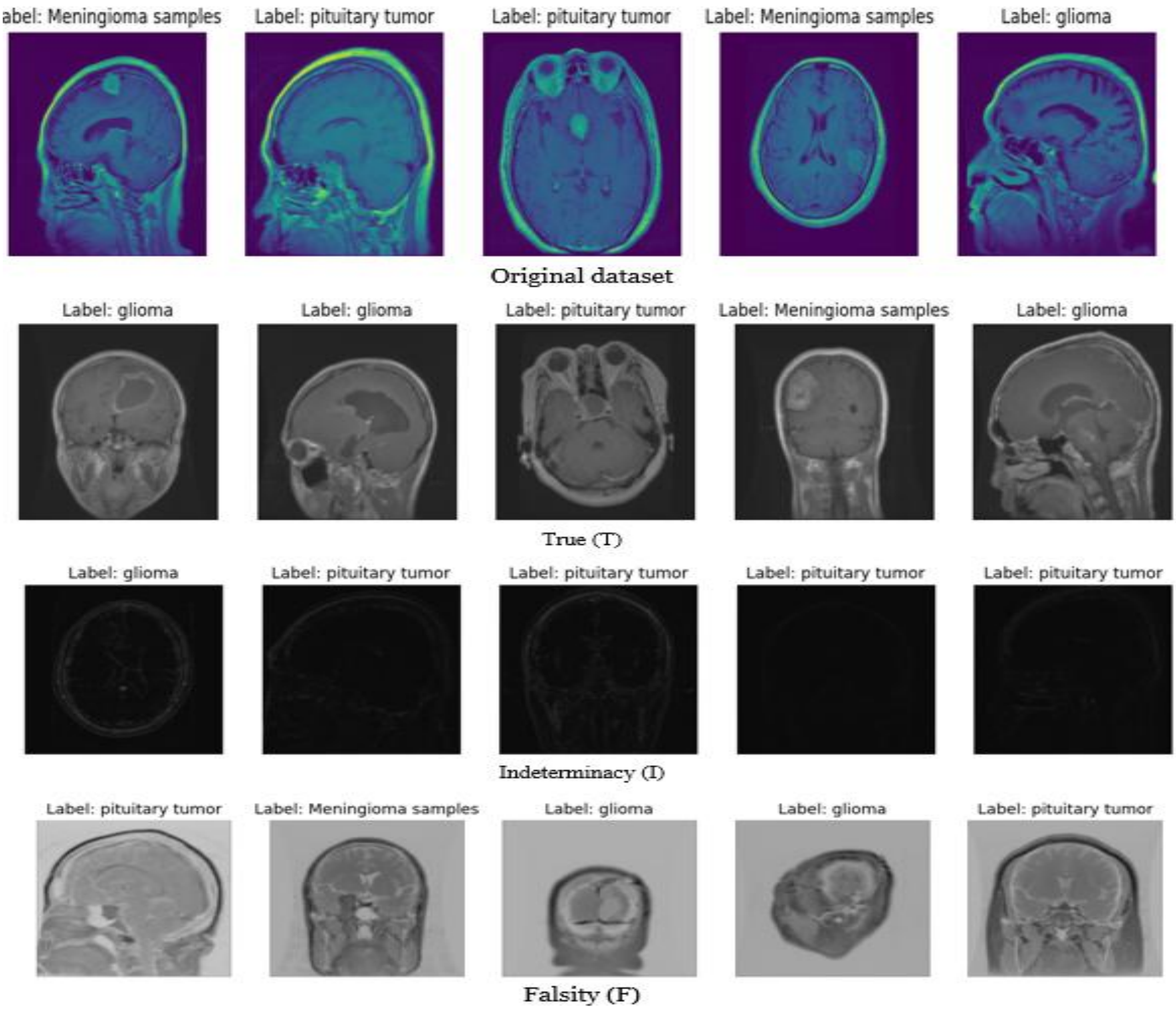


Figure 3 Different NS Images Domains Conversion Original images, True domain, Indeterminacy domain, and Falsity domain image

### *3.3 Deep learning models*

Deep learning has emerged as a strong method for addressing complicated challenges across several domains, including medical picture processing. Convolutional Neural Networks (CNNs) are pivotal in deep learning, revolutionizing image classification by extracting hierarchical feature representations from data. They examine grid-structured data, such as images, to find prominent characteristics including edges, textures, and patterns. In medical imaging, CNNs can discern intricate patterns that elude human detection, rendering them essential for illness diagnosis and fracture recognition. Transfer learning is employed to modify models for new domains, hence minimizing the requirement for substantial training data [16]. This study involves training deep learning models to operate within the neutrosophic domain, wherein medical images are converted to represent true, false, and indeterminate information based on neutrosophic sets.

By identifying these properties, the models are prepared to manage the basic uncertainty inherent in medical imaging data. Transfer learning methodologies are utilized to augment performance by fine-tuning pertained CNN models for novel medical imaging domains. Fine-tuning pertained models on medical MRI datasets enables the extraction of more relevant information related to fractures and pulmonary illnesses [17]. Numerous existing deep learning models, noted for their computational efficiency and feature extraction skills, were utilized to classify medical MRI images. These models have exhibited exceptional performance in diverse medical imaging applications and have been chosen for their demonstrated capacity to learn complex characteristics from data and their promise to tackle the complexities of classification jobs using MRI images.

Many DL models are utilized, including: MobileNetV2, VGG16, NN, Inception-V3 and DenseNet121. The fundamental architecture of MobileNetV2 is derived from its predecessor, MobileNetV1. MobileNetV2 employs Depth wise Separable Convolutions (DSC) to enhance portability, addressing the issue of information degradation in non-linear layers within convolutional blocks through Linear Bottlenecks, and introduces a novel architecture called Inverted Residuals to maintain information integrity [18]. Another DL model is VGG16 which is a neural network architecture that garnered attention during the 2014 ILSVRC (ImageNet) challenge [19].

Also, NN is classified among the premier designs for classification of images models. The model is significant for utilizing a 3x3 filter convolution while maintaining the same max pooling and padding layer as a 2x2 filter, instead of an excessive number of hyper-parameters. The organization of convolutional and max pooling layers is consistent throughout the system. Ultimately, the output comprises two completely connected softmax layers. DenseNet121 is generally used because it can improve feature reuse, solve the vanishing gradient problem, and minimize parameter use—all of which are benefits for deep learning models. Moreover, DenseNet-121 has shown performance in disease diagnosis using image databases [20].

The designation 16 in VGG16 signifies that the architecture comprises 16 layers with diverse weights, totaling around 138 million parameters [21]. Moreover, the Inception-V3 model is a development of the V1 model. Several techniques are used in the Inception-V3 model to maximize network optimization for higher model adaption. Its network is more complete than those of the V1 and V2 models. It is designed especially on a low-specification machine, the V3 model is a neural network. Training takes a lot of time and could last several days, hence it is really demanding. Transfer learning keeps the last layer of the model for new categories, therefore addressing this problem. The parameters of the previous levels remain the same; the V3 model is deconstructed by removing the last layer using the transfer learning approach [22].

## 4. Experiments and results

In this section, we will investigate the performance of several DL models, such as VGG16, DenseNet121, InceptionV3 and MobileNetV2. All models were trained using images generated through NS into T, I and F domain images, and FL into membership and non-membership images. The models employ the Adam optimizer with a learning rate of 0.001, a total of 100 epochs and a batch size of 32.

### *4.1 Experiment setup*

Using a MATLAB application, photographs were transformed to NS images; the testing with DL models was place on the Kaggle platform with GPU P100. With sixteen GB of RAM, the proposed model was built and trained using Python 3.10, Keras 3.5 and TensorFlow 2.15.

### *4.2 Evaluation metrics*

Using accuracy, precision, recall, and F1-score—mathematically defined in Eqs. (7–10)—a set of tests is conducted to evaluate the proposed model and compare it with existing state-of- the-art models.

- In machine learning, accuracy is a measure of the frequency with which a model correctly forecasts results. It is computed by dividing the number of correct forecasts by the total number of all forecasts. The correct forecasts are composed of both True Positives (TP) and True Negatives (TN) forecasts. All predictions are composed of Positive (P) and Negative (N) forecasts, where P consists of TP and False Positive (FP), and N consists of TN and False Negative (FN). It can be expressed as follows:

$$Acc = \frac{TP + TN}{TP + FP + TN + FN} \tag{6}$$

- One measure of a machine learning model's accuracy in predicting the positive class is precision. Dividing the total number of cases expected as positive by the number of genuine positives yields precision—both true and false positives included. It is mathematically formulated as:

$$\Pr ecision = \frac{TP}{TP + FP} \tag{7}$$

- Recall is a metric measuring, among all the actual positive samples in the dataset, the frequency with which a machine learning model correctly finds positive examples true positives. Dividing the total number of positive cases by the amount of true positives can help one to get recall. The latter consists in false negatives (missed cases) and true positives—accurately identified cases. The recall metric can be calculated as:

$$\operatorname{Re} call = \frac{TP}{TP + FN} \tag{8}$$

- We want both precision and recall to equal one; so, false positives and false negatives equal zero as well. We thus need a statistic that takes recall into account as well as precision. A measure combining recall and accuracy is the F1-score. It can be computed as:

$$F1\_score = 2 \times \frac{\operatorname{Re} call \times \Pr ecision}{\operatorname{Re} call + \Pr ecision} \tag{9}$$

### 4.3 *Statistical Analysis of different deep learning models*

This part analyses the performance of the transfer learning model across accuracy, precision, recall, and F1-score measurements by means of the employed picture data. Table 1 presents how well the model performed using original data. Table 2 illustrates how well the model performed on true. Table 3 presents model performance on indeterminacy. Table 4 presents how well the model performed on falsehood.

The findings of the trial showed that NS domain images obtained better test accuracy than original images. Over all experimental trials, the True (T) NS domain achieved the highest testing accuracy when compared among the T, I, and F NS domain images. Among Transfer learning models, the DenseNest121 model has shown exceptional performance in all picture categories. Table 2 shows the ideal accuracy of a model for a certain image type; DenseNet121 obtained an accuracy of 90.87%, with precision at 90.71% and recall at 90.87% for NS Domain images.

Table 1 original dataset

| Model | Accuracy | Precision | Recall | F1-score |
|---|---|---|---|---|
| **MobileNet** | 0.8783 | 0.8751 | 0.8783 | 0.8750 |
| **VGG16** | 0.8848 | 0.8824 | 0.8848 | 0.8820 |
| **InceptionV3** | 0.8674 | 0.8651 | 0.8674 | 0.8660 |
| **DenseNet121** | 0.8783 | 0.8753 | 0.8783 | 0.8748 |

Table 2 True NS

| Model | Accuracy | Precision | Recall | F1-score |
|---|---|---|---|---|
| **MobileNet** | 0.8935 | 0.8978 | 0.8935 | 0.8942 |
| **VGG16** | 0.8891 | 0.8898 | 0.8891 | 0.8891 |
| **InceptionV3** | 0.9065 | 0.9056 | 0.9065 | 0.9056 |
| **DenseNet121** | 0.9087 | 0.9071 | 0.9087 | 0.9073 |

Table 3 Indeterminacy NS

| Model | Accuracy | Precision | Recall | F1-score |
|---|---|---|---|---|
| **MobileNet** | 0.7935 | 0.7935 | 0.7717 | 0.7740 |
| **VGG16** | 0.7435 | 0.7465 | 0.7435 | 0.7240 |
| **InceptionV3** | 0.7696 | 0.7675 | 0.7696 | 0.7677 |
| **DenseNet121** | 0.8130 | 0.8147 | 0.8130 | 0.8135 |

Table 4 Falsity NS

| Model | Accuracy | Precision | Recall | F1-score |
|---|---|---|---|---|
| **MobileNet** | 0.8717 | 0.8679 | 0.8717 | 0.8656 |
| **VGG16** | 0.8391 | 0.8329 | 0.8391 | 0.8344 |
| **InceptionV3** | 0.8761 | 0.8749 | 0.8761 | 0.8745 |
| **DenseNet121** | 0.8957 | 0.8931 | 0.8957 | 0.8933 |

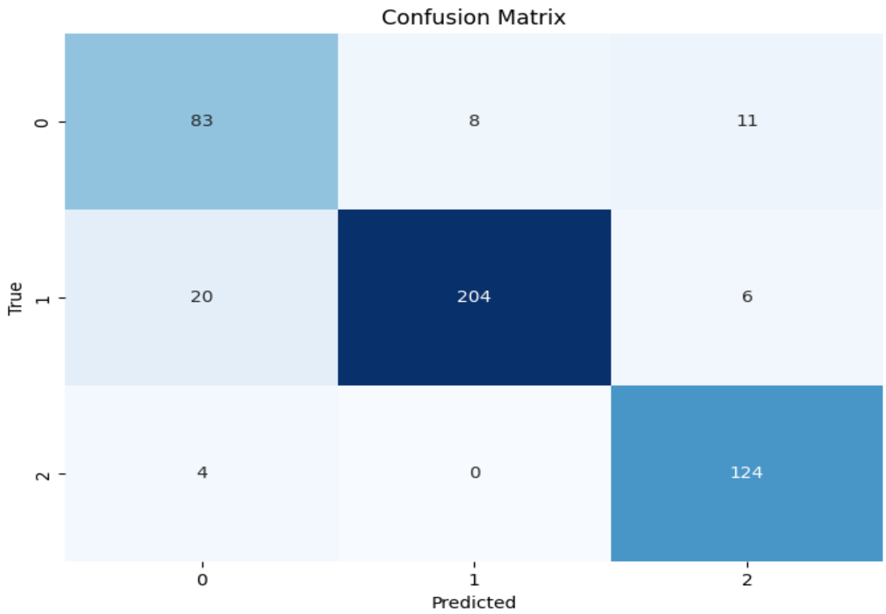


Figure 4 The confusion matrix MobileNet model on True NS

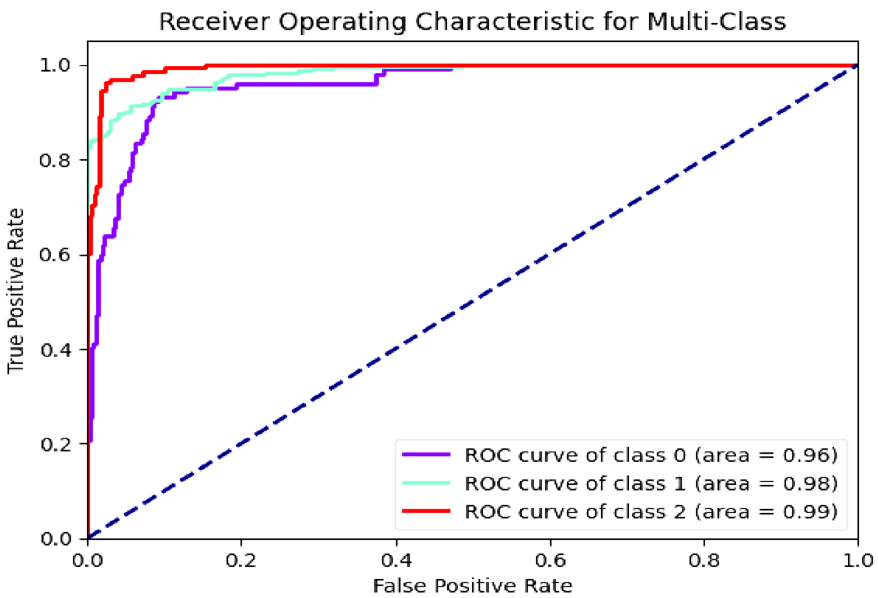


Figure 5 The ROC MobileNet model on True NS

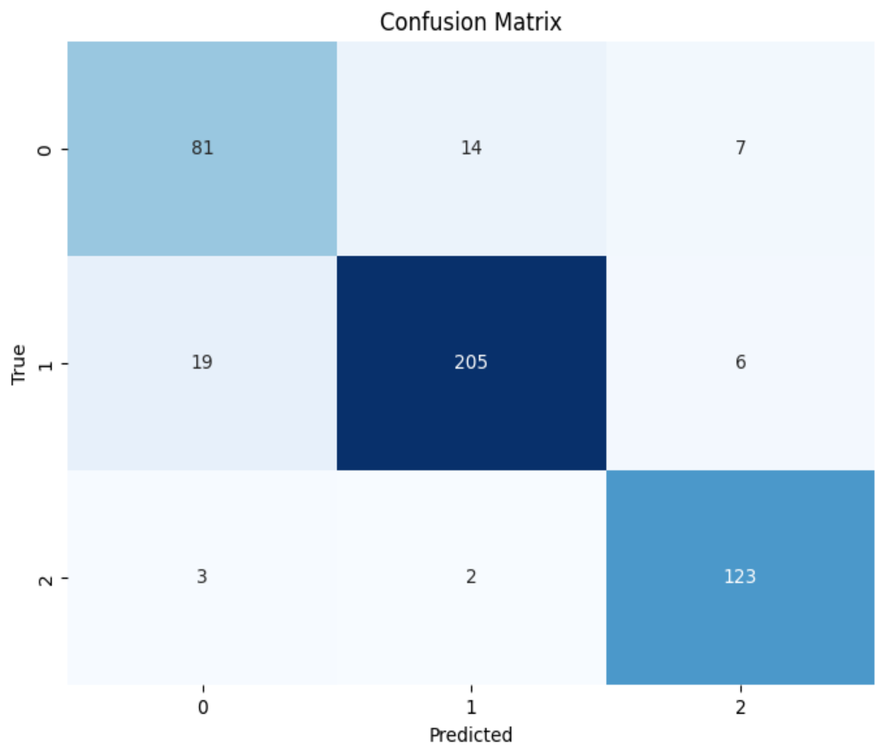


Figure 6 The confusion matrix VGG16 model on True NS

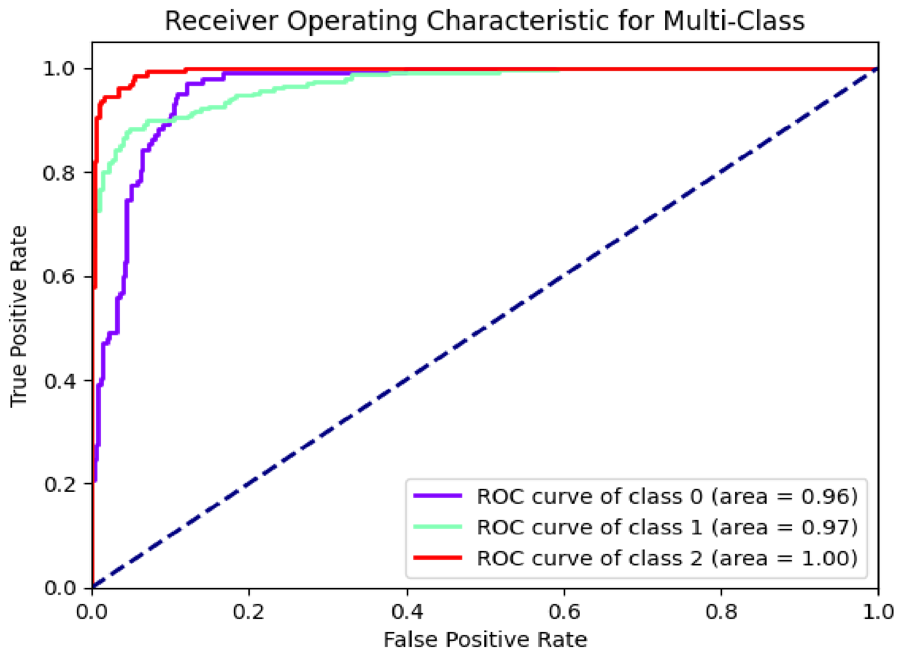


Figure 7 The ROC VGG16 model on True NS

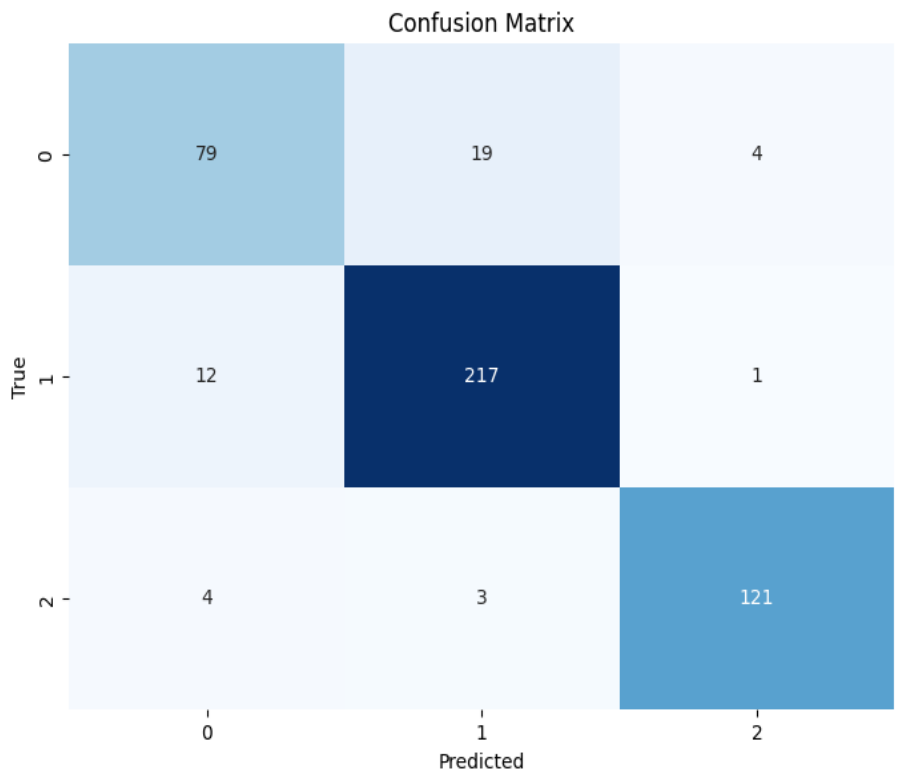


Figure 8 The confusion matrix Inception v3 model on True NS

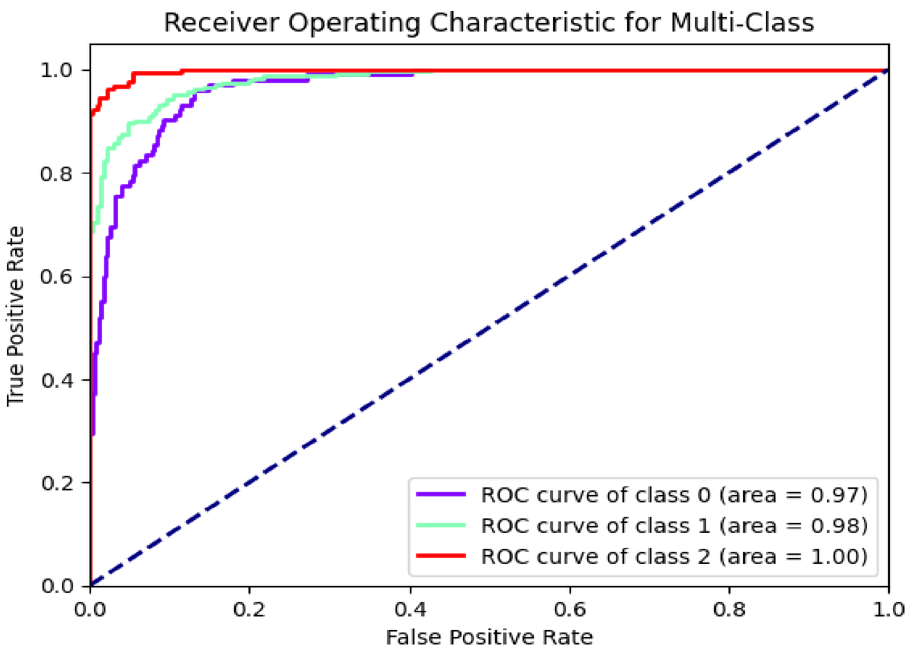


Figure 9 The ROC Inception V3 model on True NS

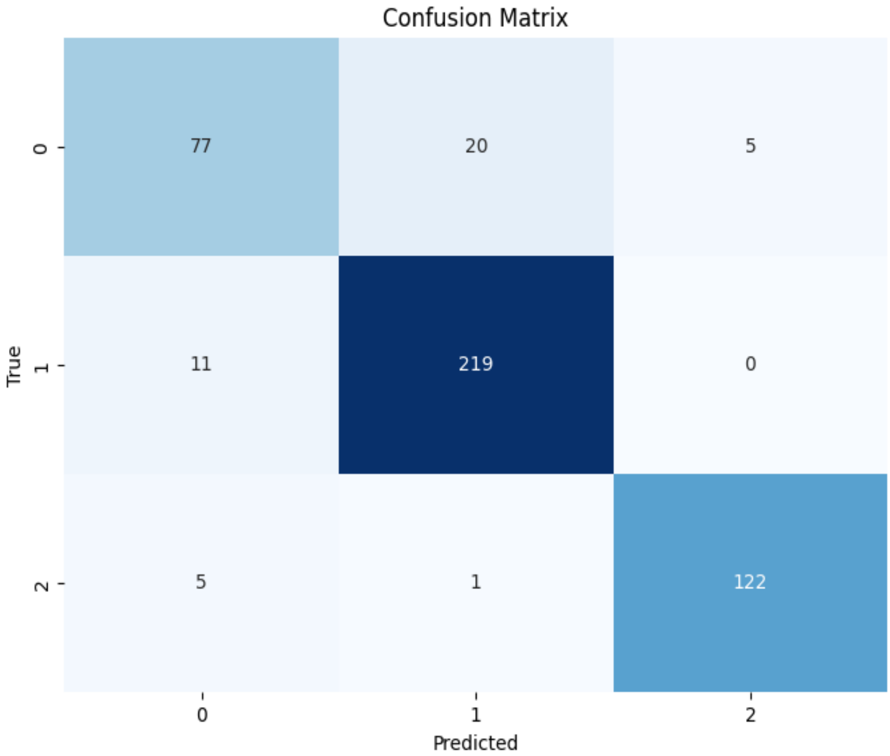


Figure 10 The confusion matrix DenseNet121 model on True NS

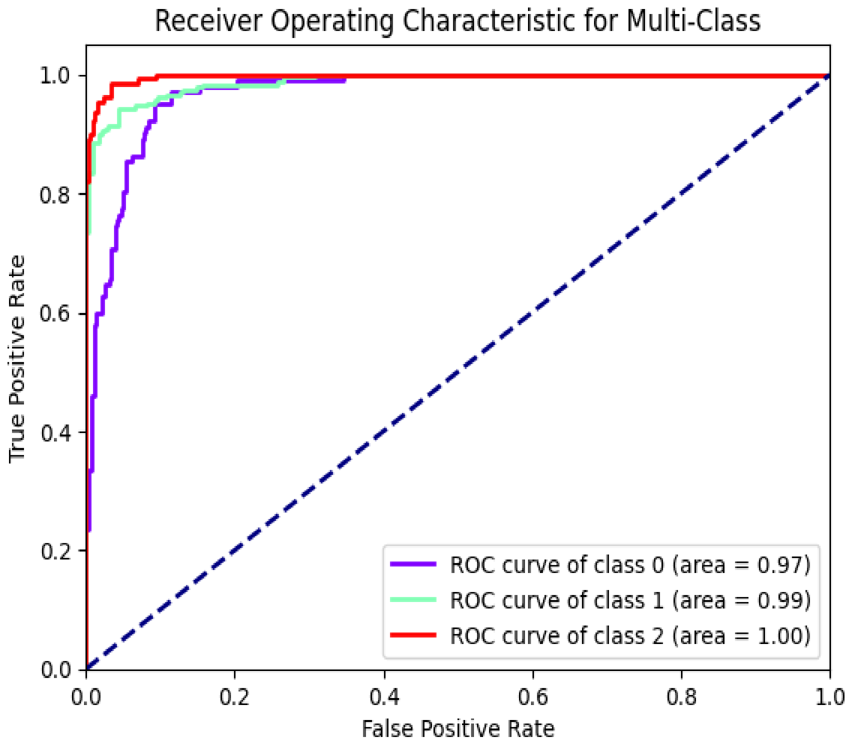


Figure 11 The ROC DenseNet121 model on True Ns

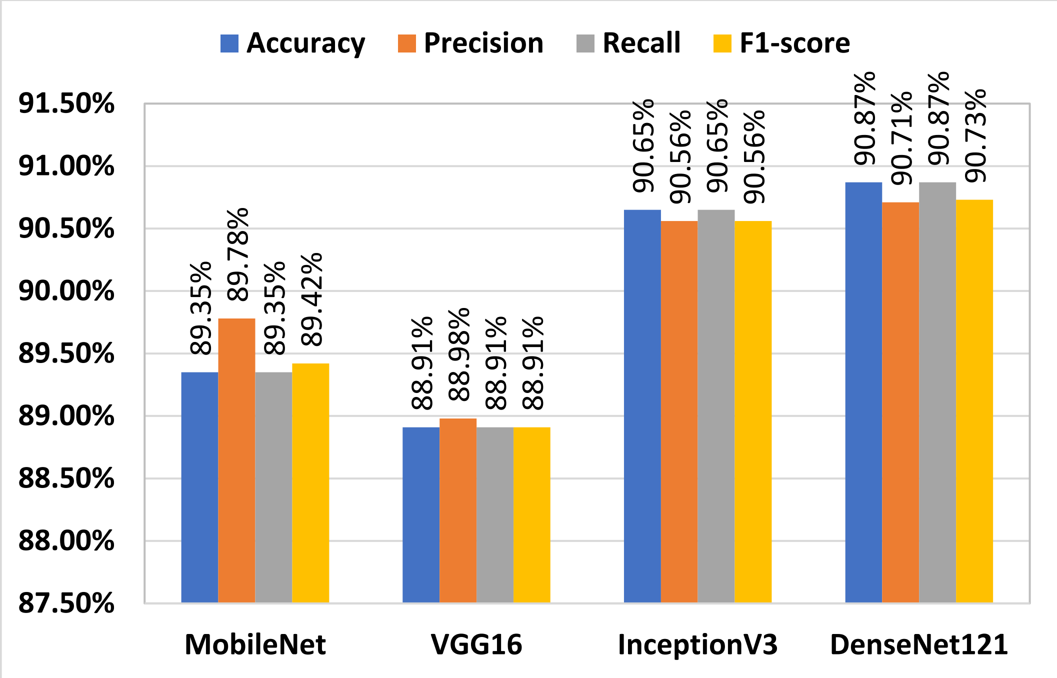


Figure 12 Performance comparisons among four models on Ns domain (True)

The application of the neutrosophic domain markedly impacts the classification accuracy and robustness of the model. Upon analyzing the confusion matrix in figure 4, figure 6, figure 8 and figure 10 of each model utilizing the neutrosophic True (T). The performance disparity demonstrates that the neutrosophic domain model attains superior classification accuracy and has a reduced incidence of misclassification. Figure 12 performs a graphical comparison among the four DL models in terms of accuracy, precision, recall and f1-score metrics. As can be shown from figure 12, DenseNet121 achieves the best results with values of 90.87%, 90.71%, 90.87% and 90.73% for accuracy, precision, recall and f1-score, respectively. On the other hand, VGG16 shows the worst performance for accuracy metric with a value of 88.91%.

## 5. Conclusion

This paper presents an exciting strategy for enhancing classification accuracy in brain tumors through the merging of NS and DL techniques. Four DL models have been created to assess their performance inside the NS domain. The NS is capable of managing uncertainty and ambiguity in higher dimensions. DL is an improved tool for categorization compared to conventional ML models. The assessment of our work has been conducted on 3,064 pictures to categorize brain tumor histology. Ultimately, the NS demonstrates higher performance regarding accuracy, precision, recall, and F1-score.

## Refernces

.1 Cheng, J., et al., *Enhanced performance of brain tumor classification via tumor region augmentation and partition.* PloS one, 2015. **10**(10): p. e0140381.

.2 Yazdani, S., et al., *Image segmentation methods and applications in MRI brain images.* IETE Technical Review, 2015. **32**(6): p. 413-427.

.3 Sadoon, T.A. and M.H. Ali, *Deep learning model for glioma, meningioma and pituitary classification.* Int. J. Adv. Appl. Sci. ISSN, 2021. **2252**(8814): p. 8814.
.4 Majumdar, P., *Neutrosophic sets and its applications to decision making*, in *Computational Intelligence for Big Data Analysis: Frontier Advances and Applications*. 2015, Springer. p. 97-115.
.5 Goguen, J.A., *LA Zadeh. Fuzzy sets. Information and control, vol. 8 (1965), pp. 338–353.-LA Zadeh. Similarity relations and fuzzy orderings. Information sciences, vol. 3 (1971), pp. 177–200.* The Journal of Symbolic Logic, 1973. **38**(4): p. 656-657.
.6 Guo, Y. and A.S. Ashour, *Neutrosophic set in medical image analysis*. 2019: Academic Press.
.7 LeCun, Y., Y. Bengio, and G .Hinton, *Deep learning.* nature, 2015. **521**(7553): p. 436-444.
.8 Bhandari, A., J. Koppen, and M. Agzarian, *Convolutional neural networks for brain tumour segmentation.* Insights into Imaging, 2020. **11**(1): p. 77.
.9 Özyurt, F., et al., *Brain tumor detection based on Convolutional Neural Network with neutrosophic expert maximum fuzzy sure entropy.* Measurement, 2019. **147**: p. 106830.
.10 Cai, G., et al., *Neutrosophic set-based deep learning in mammogram analysis*, in *Neutrosophic Set in Medical Image Analysis*. 20 ,19Elsevier. p. 287-310.
.11 Khalifa, N.E.M., et al., *A study of the neutrosophic set significance on deep transfer learning models: An experimental case on a limited covid-19 chest x-ray dataset.* Cognitive Computation, 2021: p. 1-10.
.12 Wajid, M.A., A .Zafar, and M.S. Wajid, *A deep learning approach for image and text classification using neutrosophy.* International Journal of Information Technology, 2024. **16**(2): p. 853-859.
.13 Singh, S.K., V. Abolghasemi, and M.H. Anisi, *Skin cancer diagnosis based on neutrosophic features with a deep neural network.* Sensors, 2022. **22**(16): p. 6261.
.14 Cheng, J., *Brain Tumor Image Dataset*, https://doi.org/10.6084/m9.figshare.1512427.v5, Editor. 2017.
.15 Smarandache, F., *A unifying field in Logics: Neutrosophic Logic* ,in *Philosophy*. 1999, Citeseer. p. 1-141.
.16 Krizhevsky, A., I. Sutskever, and G.E. Hinton, *Imagenet classification with deep convolutional neural networks.* Advances in neural information processing systems, 2012. **25**.
.17 Torrey, L. and J. Shavlik, *Transfer learning*, in *Handbook of research on machine learning applications and trends: algorithms, methods, and techniques*. 2010, IGI global. p. 242-264.
.18 Dong, K., et al. *MobileNetV2 model for image classification*. in *2020 2nd International Conference on Information Technology and Computer Application (ITCA)*. 2020. IEEE.
.19 El Asnaoui, K., Y. Chawki, and A. Idri, *Automated methods for detection and classification pneumonia based on x-ray images using deep learning*, in *Artificial intelligence and blockchain for future cybersecurity applications*. 2021, Springer. p. 257-284.
.20 Torky, M., et al., *Deep learning model for recognizing monkey pox based on dense net-121 algorithm.* medRxiv, 2022: p. 2022.12. 20.22283747.
.21 Hammoudi, K., et al., *Deep learning on chest X-ray images to detect and evaluate pneumonia cases at the era of COVID-19.* Journal of medical systems, 2021. **45**(7): p. 75.
.22 Mujahid, M., et al., *Pneumonia classification from X-ray images with inception-V3 and convolutional neural network.* Diagnostics, 2022. **12**(5): p. 1280.

Received: Oct 9, 2024. Accepted: March 24, 2025